ISSN: 2096-3246
Volume 58, Issue 01, 2026

ANALYSIS AND EVALUATION OF THE SHIELDING CHARACTERISTICS OF PR_2O_3 DOPED SODIUM LEAD-BORATE GLASSES FOR GAMMA RAY SHIELDING APPLICATIONS.

Susheela K Lenkennavar[1,2] and B. M. Praveen[1*]
[1]Department of Chemistry, Institute of Engineering and Technology, Srinivas University, Mukka, Mangaluru, Karnataka 574146, India.
[2]Department of Physics, Bangalore University, Bengaluru, Karnataka-560056, India.
*Corresponding author. E-mail address: bm.praveen@yahoo.co.in

Abstract A new set of glass samples consisting of $30Na_2O$-5PbO-$5PbF_2$-10BaO-(60-x)B_2O_3-x Pr_2O_3, with $0 \leq x \leq 0.5$, was synthesised using the melt quench technique. The radiation attenuation characteristics of the produced glasses were analyzed using Phy-X/PSD software. The values of μ increased from 0.015 MeV, where the MAC values are 37.008 cm^2/g and 37.522 cm^2/g for BaO at 10 mol% with Pr_2O_3 at 0% and 0.5%, respectively. The HVL value for BaO-Pr-0.0 glass was measured at 3.702 cm when subjected to 1.5 MeV, and BaOPr-0.5 glass demonstrated HVL values of 4.069 cm at the same photon energy level. The MFP values measured reflect HVL characteristics, indicating that BPr-5.0 glass provides superior values across different photon energies when assessed against the other prepared glasses. Among the tested materials, prepared glasses reveal enhanced shielding effectiveness when juxtaposed with commonly utilized glass and concrete samples. The findings of this study highlight the feasibility of these glass types as practical solutions for shielding against gamma radiation.
Keywords: Lead-borate glasses, Gamma ray shielding, Mass attenuation coefficient, Half value layer. Mean free path.

1. Inroduction

High-energy ionizing radiations such as X-rays and gamma rays are widely employed in fields like medicine, industry, and agriculture. Despite their usefulness, these radiations pose serious risks to living beings, the surrounding environment, and sensitive electronic equipment, mainly due to their highly penetrating neutral nature. Therefore, reducing the intensity of such radiation through appropriate shielding remains the most reliable approach for minimizing their harmful effects [1, 2].

The Fukushima nuclear accident in Japan has renewed global attention toward the use of radiation and the importance of protective materials in radiological engineering, science, and technology. Several types of radiation—including gamma rays, X-rays, alpha particles, beta particles, and neutrons—are commonly produced and utilized in nuclear medicine, radiotherapy, and nuclear reactor systems. Gamma rays and X-rays, being massless, can propagate over long distances in air. Similarly, neutrons are capable of traveling significant distances due to their neutral charge. Due to this property, gamma rays, X-rays, and neutrons are among the most deeply penetrating forms of radiation, which makes effective shielding particularly difficult [3]. In practice, lead is commonly used to attenuate X-rays and gamma rays, whereas neutron radiation typically requires much thicker shielding, such as concrete

barriers with thicknesses on the order of one meter [4, 5]. Protection against radiation is essential for people working in environments where radiation exposure is possible. As a result, many researchers have examined different shielding techniques and materials to improve radiation safety. Al-Buriahi et al. have shown that certain polymers can offer effective shielding performance and may be useful for radiation protection applications [6].

Radiation shielding characteristics of a certain medium depend on its composition and density. Moreover, the thickness of the medium is another element that affects its shielding capabilities [7-10]. The cost-effectiveness of glass, combined with the numerous preparation methods, the ability to create glass samples in different thicknesses and shapes, and importantly, the superior radiation shielding factors, make glass an attractive option for shielding purposes [11-15]. Glass that includes heavy metal (HM) oxides like PbO provides outstanding protection against gamma rays. Its high density and the elevated effective atomic number of each component in the glass composition result in low relaxation times and half-layer values [16].

Lead glass is commonly used for the purpose of radiation shielding. Different types of lead glass have been applied in medical institutions for screens, windows, doors, and walls. Lead glass is typically found in radiation facilities, hot cells, laboratories, and radioactive storage sites. Additionally, it is used in fuel development and for various applications related to nuclear reactors. This is attributed to the properties of lead glasses, which offer both transparency and effective attenuation of high-energy photons [17].

The effectiveness of radiation shielding materials is influenced by various physical parameters such as the half value layer (HVL), effective atomic number (Z_{eff}), mass attenuation coefficient (μ/ρ), transmission factor, mean free path (MFP). The main focus of this investigation is to provide insight into the optical features and γ-ray shielding factors of NPPBP glasses. The radiation attenuation characteristics of the produced glasses were analyzed using Phy-X/PSD software. The expected results of this investigation will feature enhanced compositions of the target glass system, meticulously crafted to provide optimal radiation-shielding capabilities. The expectation is that the findings of this study will contribute to the advancement of materials designed for a range of applications in the field, with the goal of protecting those who are in close contact with radiation-emitting sources. The importance of the current research lies in its focus on broadening the area of radiation-attenuating materials. By highlighting the fundamental properties and potential provided by the Na_2O-PbO-PbF_2-BaO-B_2O_3-Pr_2O_3 (NPPBP) glass system,

2. Materials and methods

2.1 Glasses preparation

The selected glass samples were fabricated utilizing the well-known melt quenching method. In total, five glass samples with a nominal composition of $30Na_2O$-5PbO-$5PbF_2$-10BaO-(60-x)B_2O_3-x Pr_2O_3 (x=0, 0.1, 0.3, 0.5 mol%) were created from the chemical powders Na_2O, PbO, PbF_2, B_2O_3, Pr_2O_3, and BaO. Furthermore, glasses were also produced using other metal oxides like CaO and SrO. Once the essential chemicals were measured, a 10 g sample of each glass powder was mixed thoroughly. It was then subjected to melting for 40 minutes at 1000°C in a high-temperature electric furnace with a high-purity porcelain crucible. To reduce internal

stresses, the glass samples were heated in another furnace for 1 hours at 400 °C during the annealing process.

2.2 Theoretical analysis conducted using Phys-X software.

The radiation shielding factors for the synthesized NPPBP samples were evaluated using Phy-X software [18] at the identical energies applied in the experimental study. Phy-X is a practical tool for evaluating the radiation shielding factors for any chosen glass system. It can be applied to effectively showcase the radiation shielding performance of materials against both low and high energy photons. Evaluating these attenuation factors enhances our insight into the radiation shielding performance of these glasses.

The Lambert-Beer law serves as a primary equation to illustrate the reduction in intensity of a radiation beam as it moves through a particular substance. This equation can be mathematically represented as [19, 20]:

$I = I_0\, e^{-\mu x}$ (1)

In the equation presented above, I_0 and I represent the unabated and attenuated intensities of the photon, respectively, while μ signifies the linear attenuation coefficient (LAC). The equation mentioned above can be rewritten as :

$MAC = \frac{1}{\rho x} \ln\left(\frac{I_0}{I}\right)$ (2)

In the case of certain mediums, the MAC is a significant parameter as it enables us to estimate the LAC for that medium. Essentially, we can link the MAC and LAC for a medium using equation 3 [21] :

LAC = MAC × density (3)

The half value layer (HVL) indicates the thickness of an absorber that lowers the intensity of incoming radiation by 50%. Namely [22, 23]:

$HVL = \frac{ln2}{LAC}$ (4)

3. Results and Discussion

Radiation Shielding Properties of the NPPBP Glasses

The Phy-X software was used to determine the radiation shielding factors for the NPPBP samples that incorporated different metal oxides. The Phy-X software [18, 24] effectively calculates radiation shielding factors for various glass systems. It is particularly beneficial for evaluating the shielding properties of materials against both low and high-energy photons. One of the primary benefits of Phy-X is its user-friendly interface, which enables easy input of the glass composition and density on the main page [25]. This straightforwardness, coupled with the program's accuracy, makes it an indispensable resource for researchers and professionals in the field. Users can provide the glass composition in either mol% or wt%, and the density should be indicated in g/cm^3. Additionally, the user must select the energy range for testing the samples. In this analysis, energies were specified within the range of 0.015 MeV to 15 MeV.

The examination of the radiation shielding features of the NPPBP glass samples involved scrutinising important shielding parameters across the photon energy range of 0.015–15 MeV. This analysis was conducted using the Windows-based Phy-X software to determine the

radiation shielding parameters applicable to the NPPBP glass compositions. A key metric in radiation physics, the mass attenuation coefficient (MAC) measures the extent to which a substance can attenuate (absorb or scatter) a photon beam (such as X-rays or gamma rays) per unit mass [26-28]. It provides an understanding of how effectively a material can attenuate the strength of radiation that passes through it.

The mass attenuation coefficient (MAC), which is quantified in cm^2/g, signifies the probability of photon interaction with a given material. Figure 3 depicts the association between MAC values and energy. It is clear that when the γ photon attains 1 MeV, the MAC values drop rapidly. This reduction is due to photoelectric absorption. This effect is particularly important at lower photon energy levels. It is widely recognised that the absorption cross-section associated with the photoelectric effect changes with the atomic number of the material, represented as $Z^{4.5}$, and the energy of the primary photon, denoted as $E^{-3.5}$. Therefore, the MAC values for the glasses being studied and the materials being compared are highest in the low energy range.

The analysis demonstrated that the highest MAC values for all NPPBP samples were found at 0.015 MeV, with a subsequent sharp decrease as photon energy increased. In the first region, within the initial gamma energy range of 0.015-0.02 MeV, the MAC values decline as the concentration of Pr_2O_3 increases, primarily due to the dominant photoelectric effect. At 0.015 MeV, the MAC values are 37.008 cm^2/g and 37.522 cm^2/g for BaO at 10 mol% with Pr_2O_3 at 0% and 0.5%, respectively. For CaO at 10 mol%, the values are 28.628 cm^2/g and 29.363 cm^2/g for Pr_2O_3 at 0% and 0.5%, respectively. Lastly, for SrO at 10 mol%, the MAC values are 27.206 cm^2/g and 27.891 cm^2/g for Pr_2O_3 at 0% and 0.5%, respectively.

In addition, the gradual reduction of MAC observed with the increase in photon energy in the 0.1–1 MeV range can be explained by the Compton Scattering (CS) process, which is characterised by its cross-sectional dependence on the ratio of atomic number to photon energy (Z/E). In Figure 1 and figure 2, the correlation between MAC values and energy is depicted. It is apparent that as the γ photon approaches 1 MeV, there is a swift decline in MAC values. This decline is due to photoelectric absorption.

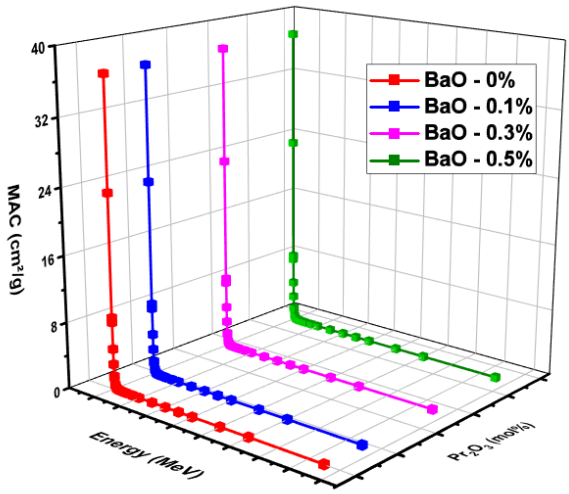

Fig. 1. Mass attenuation coefficients (μ/ρ) of the investigated glasses as a function of the photon energy-Ba_2O Incorporated glasses.

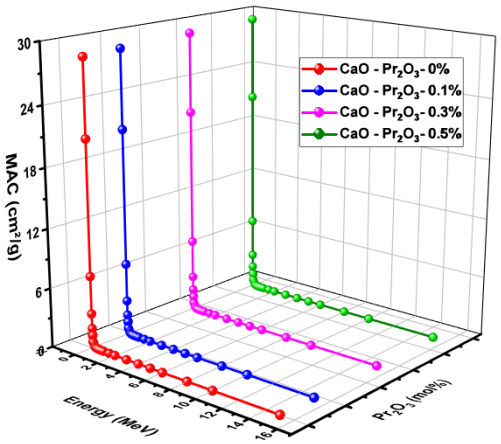

Fig. 2. Mass attenuation coefficients (μ/ρ) of the investigated glasses as a function of the photon energy-CaO incorporated glasses.

Across the energy range of (0.15–0.4 MeV), the values sharply decline to about 0.127 (cm^2/g), then gradually reduce to approximately 0.089 (cm^2/g) in the (0.4–0.6 MeV) range, and finally show an insignificant decrease in the (0.662–1.5 MeV) range of BaO incorporated glasses. In the energy range of (0.15–0.4 MeV), the values significantly drop to about 0.125 (cm^2/g), then slowly decrease to nearly 0.089 (cm^2/g) in the (0.4–0.6 MeV) range, and finally show a minor decline in the (0.662–1.5 MeV) range of CaO incorporated glasses. Similarly, in the energy range of (0.15–0.4 MeV), the values sharply fall to approximately 0.122 (cm^2/g), then gradually diminish to around 0.088 (cm^2/g) in the (0.4–0.6 MeV) range, and ultimately reveal an insignificant drop in the (0.662–1.5 MeV) range of SrO incorporated glasses.

Half value layer (HVL) and mean free path (MFP).

Fig. 3 depict the variation in HVL and MFP in the Pr_2O_3-doped Sodium-Lead boro lead fluride glass system as a function of the energy of the incident photons

The HVL of NPPBP glasses containing BaO, SrO, and CaO is illustrated in Fig. 3 as a function of energy. A significant metric for any shielding material is the HVL, which is the thickness required to reduce the photon-beam intensity by half as it passes through the material. Therefore, selecting lower values is advisable for identifying the most effective γ-ray shielding composition.

For BaO-Pr-0.0 glass, the HVL value was found to be 3.702 cm at 1.5 MeV. Meanwhile, BaOPr-0.5 glass has shown HVL values of 4.069 cm at the same photon energy. In addition, CaO-Pr-0.5 glass reached HVL values of 4.265 cm at ~1.5 MeV, and SrO-Pr-0.5 glass also achieved HVL values of 3.898 cm at ~1.5 MeV. The lowest HVL value of BaO-Pr-0.0 glass highlights its superior shielding capabilities compared to all other glasses produced.

The MFP values obtained exhibit HVL characteristics, indicating that BPr-5.0 glass demonstrates superior values across various photon energies when compared to the other prepared glasses.

Our prepared glass (BPr-5.0) exhibits the highest MFP values across all photon energy levels. This characteristic renders our glass system more effective than that of our competitors in terms of γ-ray shielding. Furthermore, our sodium-leadborate glass system doped with presodium

outperforms standard concrete, barite concrete, and commercial glass (RS 360) in terms of γ-ray protection. In the interval of 0.1–5 MeV, HVL values experience a rapid increase due to secondary scatterings and the rising photon energy. Conversely, HVL values from 6 to 15 MeV are relatively stable and are not influenced by the concentration of the glasses.

For the NPPBP0 glass with BaO-10%, the HVL values at 15 MeV are 5.807 cm, while for the NPPBP0.5 glass, they are 6.336 cm. Similarly, the HVL values at 15 MeV for the NPPBP0.5 glass with CaO-10% are 7.828 cm, and for the NPPBP0.5 glass with SrO-10%, they are 6.679 cm. Increasing the substitution of Pr_2O_3 has resulted in a reduction of the glass thickness necessary to attenuate gamma photons.

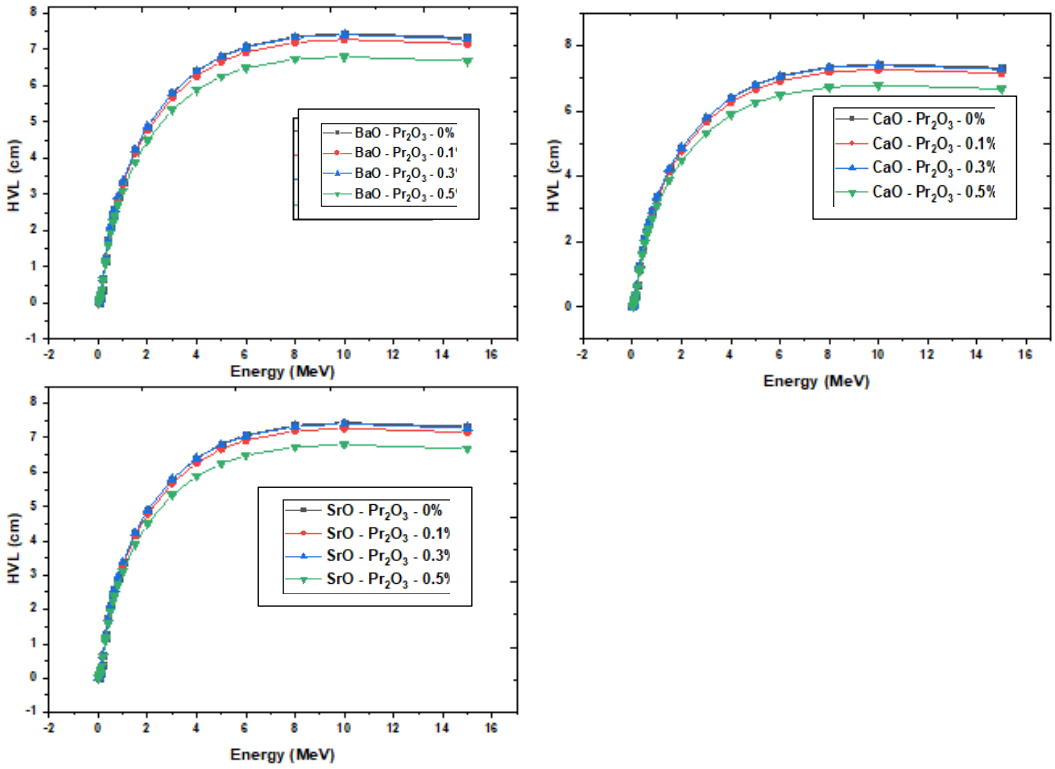

***Fig. 3**. Changes in the number of half-value layers versus incident photon energy*

Effective atomic numbers (Z_{eff})

Just as the atomic number identifies elements, the effective atomic number (Z_{eff}) serves as a crucial parameter for characterising composite materials. Similar to the mass attenuation coefficient (MAC), Z_{eff} is influenced by various microscopic photon interaction processes, such as the photoelectric effect (PE), Compton scattering (CS), and pair production (PP). As a result, it is utilised to assess the shielding properties of composite materials. The effective atomic number (Z_{eff}) of all the glasses analyzed is shown in Figure 4, revealing consistent patterns.

In this study, the Z_{eff} values for all the prepared glass compositions were determined experimentally at various photon energies. Similar to the MAC, the Z_{eff} values exhibit a significant decline in the low-energy region (0.15–0.5 MeV) because the PE process predominates in this energy range, where the interaction cross section inversely correlates with photon energy.

In the intermediate energy range, the dominance of the CS process corresponds to the lowest Z_{eff} values observed in our glasses. These values diminish as the g-photon energy increases, reaching a minimum of approximately 11.82 (e-/atom) at 1.5 MeV.

It has been noted that a low concentration of Pr_2O_3 leads to an increase in Z_{eff} values (particularly at lower photon energies), thereby enhancing the glass's shielding effectiveness.

Among all the glasses produced, BaO-NPPBPr-0.0 exhibited the highest Z_{eff} values, while NPPBPr-0.5, which included SrO, recorded the lowest values across the entire selected energy range due to the presence of Pr_2O_3. Specifically, at an energy of 0.015 MeV, the Z_{eff} for BaO-NPPBP0 glass is 56.25, and at 0.02 MeV, it is 61.23. In contrast, for BaO-NPPBP0.5, the Z_{eff} values at 0.015 and 0.02 MeV are 56.32 and 61.20, respectively.

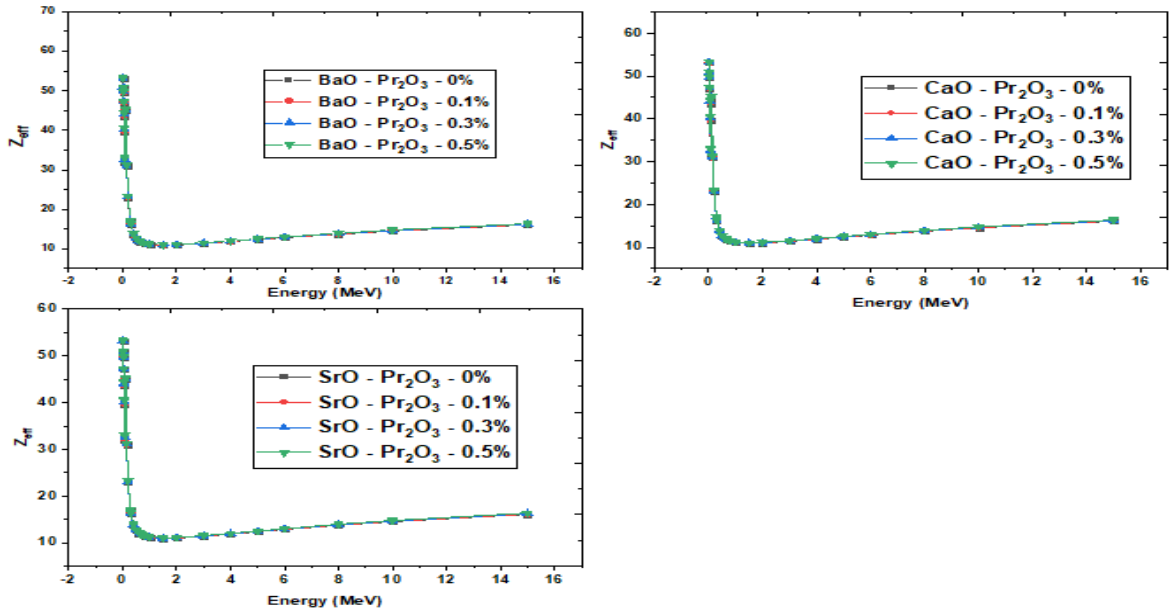

Fig. 4. The variation in effective atomic number (Z_{eff}) for the Pr_2O_3 0%, Pr_2O_3 0.1%, Pr_2O_3 0.3%, and Pr_2O_3 0.5% $Na_2O+B_2O_3+PbO+PbF_2+Pr_2O_3$ glass systems, which are combined with BaO, CaO, and SrO, is examined as a function of incident photon energy (MeV).

The last parameter we evaluate concerning radiation shielding is the linear attenuation coefficient (LAC). It is essential to note that high LAC values for certain media indicate a strong ability to impede incoming photons. Consequently, this is vital for the advancement of effective shielding glass materials. The reduction in LAC values is associated with an increase in Pr_2O_3 concentration. At approximately 0.015 MeV, the LAC for all the manufactured glasses achieved its peak values, which ranged from 139.119 cm^{-1} to 128.401 cm^{-1} for BaO-NPPBPr0 and BaO-NPPBPr0.5, respectively.

Conclusion

Using a conventional melt-quenching method, sodium lead borate glasses were synthesised with various concentrations of praseodymium oxide (Pr_2O_3). The density (ρ) of these glasses decreases as the amount of Pr_2O_3 increases.

The results indicate that the highest MAC values were observed at an energy level of approximately 0.015 MeV for all the glasses that were prepared. In addition, the gamma photon shielding parameters, including HVL, MFP, Z_{eff}, and Neff of the prepared glasses, were calculated from measurements. The findings highlight that the BaO-NPPBPr-0.0 glass exhibits

the lowest HVL and MFP values while having the highest Z_{eff} values. It is important to note that the shielding effectiveness of BaO-NPPBPr glasses against gamma photons remains unchanged with the addition of Pr_2O_3. The effect of Pr_2O_3 content on the gamma photon shielding properties of the prepared glasses is particularly pronounced at lower photon energy. The results indicate that BaO-NPPBPr-0.0 glass exhibits the highest Z_{eff} value, while CaO-NPPBPr-0.5 shows the lowest due to a significant decrease in Pr_2O_3 content. Consequently, the assessment of shielding parameters suggests that BaO-NPPBPr-0.0 glass is more effective for gamma radiation shielding than other conventional materials, such as concrete and the glasses discussed in this article.

Acknowledgement

The author (SKL) acknowledges financial support from the Vision Group on Science and Technology (VGST), Government of Karnataka, under KSTEPS/VGST/ECRA/GRD No. 1251/2023-24.

References

1. Jalali, M., & Mohammadi, A. (2008b). Gamma ray attenuation coefficient measurement for neutron-absorbent materials. Radiation Physics and Chemistry, 77(5), 523–527. https://doi.org/10.1016/j.radphyschem.2007.12.014

2. Chanthima, N., & Kaewkhao, J. (2013). Investigation on radiation shielding parameters of bismuth borosilicate glass from 1keV to 100GeV. Annals of Nuclear Energy, 55, 23–28. https://doi.org/10.1016/j.anucene.2012.12.011

3. Almatari, M. (2019). Gamma radiation shielding properties of glasses within the TeO_2-TiO_2-ZnO system. Radiochimica Acta, 107(6), 517–522. https://doi.org/10.1515/ract-2018-3058

4. Holmberg, O., Czarwinski, R., & Mettler, F. (2010). The importance and unique aspects of radiation protection in medicine. European Journal of Radiology, 76(1), 6–10. https://doi.org/10.1016/j.ejrad.2010.06.031

5. Alenezi, M., Stinson, K., Maqbool, M., & Bolus, N. (2018). Klein–Nishina electronic cross-section, Compton cross sections, and buildup factor of wax for radiation shielding and protection. Journal of Radiological Protection, 38(1), 372–381.https://doi.org/10.1088/1361-6498/aaa57b

6. Al-Buriahi, M. S., Eke, C., Alomairy, S., Yildirim, A., Alsaeedy, H. I., & Sriwunkum, C. (2021). Radiation attenuation properties of some commercial polymers for advanced shielding applications at low energies. Polymers for Advanced Technologies, 32(6), 2386–2396. https://doi.org/10.1002/pat.5267

7. Dong, M., Xue, X., Yang, H., & Li, Z. (2017). Highly cost-effective shielding composite made from vanadium slag and boron-rich slag and its properties. Radiation

Physics and Chemistry, 141, 239–244.https://doi.org/10.1016/j.radphyschem.2017.07.023

8. Dong, M., Xue, X., Yang, H., Liu, D., Wang, C., & Li, Z. (2016). A novel comprehensive utilization of vanadium slag: As gamma ray shielding material. Journal of Hazardous Materials, 318, 751–757.https://doi.org/10.1016/j.jhazmat.2016.06.012

9. Yasmin, S., Khandaker, M. U., Barua, B. S., Mustafa, M. N., Chowdhury, F.-U.-Z., Rashid, M. A., & Bradley, D. A. (2018). Ionizing radiation shielding effectiveness of decorative building materials (porcelain and ceramic tiles) used in Bangladeshi dwellings. Indoor and Built Environment, 28(6), 825–836.https://doi.org/10.1177/1420326x18798883

10. Aygün, B., Alaylar, B., Turhan, K., Şakar, E., Karadayı, M., Al-Sayyed, M. I. A., Pelit, E., et al. (2020). Investigation of neutron and gamma radiation protective characteristics of synthesized quinoline derivatives. International Journal of Radiation Biology, 96(11), 1423–1434.https://doi.org/10.1080/09553002.2020.1811421

11. Al-Buriahi, Bakhsh, E. M., Tonguc, B., & Khan, S. B. (2020). Mechanical and radiation shielding properties of tellurite glasses doped with ZnO and NiO. Ceramics International, 46(11), 19078–19083. https://doi.org/10.1016/j.ceramint.2020.04.240

12. Buriahi, A.-, Tonguç, B., Perişanoğlu, U., & Kavaz, E. (2020). The impact of Gd_2O_3 on nuclear safety proficiencies of TeO_2–ZnO–Nb_2O_5 glasses: A GEANT4 Monte Carlo study. Ceramics International, 46(15), 23347–23356. https://doi.org/10.1016/j.ceramint.2020.03.110

13. Al-Buriahi, M. S., Taha, T. A., Alothman, M. A., Donya, H., & Olarinoye, I. O. (2021). Influence of WO_3 incorporation on synthesis, optical, elastic and radiation shielding properties of borosilicate glass system. The European Physical Journal Plus, 136(7). https://doi.org/10.1140/epjp/s13360-021-01790-5

14. Alzahrani, J. S., Kavas, T., Kurtulus, R., Olarinoye, I. O., & Al-Buriahi, M. S. (2021). Physical, structural, mechanical, and radiation shielding properties of the PbO–B_2O_3–Bi_2O_3–ZnO glass system. Journal of Materials Science Materials in Electronics, 32(14), 18994–19009. Retrieved from https://doi.org/10.1007/s10854-021-06414-3

15. Abouhaswa, A. S., Mhareb, M. H. A., Alalawi, A., & Al-Buriahi. (2020). Physical, structural, optical, and radiation shielding properties of B_2O_3- 20Bi_2O_3- 20Na_2O_2-Sb_2O_3 glasses: Role of Sb_2O_3. Journal of Non-Crystalline Solids, 543, 120130. https://doi.org/10.1016/j.jnoncrysol.2020.120130

16. Zhang, X., Chen, Q., & Zhang, S. (2021). Ta_2O_5 nanocrystals strengthened mechanical, magnetic, and radiation shielding properties of heavy metal oxide glass. Molecules, 26(15), 4494. https://doi.org/10.3390/molecules26154494

17. Osman, A. M., El-Sarraf, M. A., Abdel-Monem, A. M., & Abdo, A. E.-S. (2015). Studying the shielding properties of lead glass composites using neutrons and gamma rays. Annals of Nuclear Energy, 78, 146–151. https://doi.org/10.1016/j.anucene.2014.11.046

18. Şakar, E., Özpolat, Ö. F., Alım, B., Sayyed, M. I., & Kurudirek, M. (2019). Phy-X / PSD: Development of a user friendly online software for calculation of parameters relevant to radiation shielding and dosimetry. Radiation Physics and Chemistry, 166, 108496. https://doi.org/10.1016/j.radphyschem.2019.108496

19. Akkurt, I., & Malidarre, R. B. (2021). Gamma photon-neutron attenuation parameters of marble concrete by MCNPX code. Radiation Effects and Defects in Solids, 176(9–10), 906–918.https://doi.org/10.1080/10420150.2021.1975708

20. Hussein, E. M. A., Elaziz, T. D. A., & El-Alaily, N. A. (2019). Effect of gamma radiation on some optical and electrical properties of lithium bismuth silicate glasses. Journal of Materials Science Materials in Electronics, 30(13), 12054–12064. https://doi.org/10.1007/s10854-019-01563-y

21. Mansy, M. S., Ghobashy, M. M., & Aly, M. I. (2024). Enhancing gamma and neutron radiation shielding efficiency of LDPE/PVC polymers using cobalt, aluminum, and magnesium oxide fillers. Radiation Physics and Chemistry, 222, 111862. https://doi.org/10.1016/j.radphyschem.2024.111862

22. Ekinci, N., Mahmoud, K. A., Aygün, B., Hessien, M. M., & Rammah, Y. S. (2022). Impacts of the colemanite on the enhancement of the radiation shielding capacity of polypropylene. Journal of Materials Science Materials in Electronics, 33(25), 20046–20055. https://doi.org/10.1007/s10854-022-08822-5

23. Kassem, S. M., Maksoud, M. I. a. A., Sayed, A. M. E., Ebraheem, S., Helal, A. I., & Ebaid, Y. Y. (2023). Optical and radiation shielding properties of PVC/$BiVO_4$ nanocomposite. Scientific Reports, 13(1), 10964. https://doi.org/10.1038/s41598-023-37692-y

24. Zakaly, H. M., Abouhaswa, A. S., Issa, S. a M., Mostafa, M. Y. A., Pyshkina, M., & El-Mallawany, R. (2020). Optical and nuclear radiation shielding properties of zinc borate glasses doped with lanthanum oxide. Journal of Non-Crystalline Solids, 543, 120151. https://doi.org/10.1016/j.jnoncrysol.2020.120151

25. D. A. Aloraini, A. H. Almuqrin, M. I. Sayyed, A. Kumar, D. Gaikwad, D. I. Tishkevich, and A. Trukhanov, "Experimental and theoretical analysis of radiation shielding properties of strontium-borate-tellurite glasses," Opt. Mater. 121, 111589 (2021). https://doi.org/10.1016/j.optmat.2021.111589.
26. Alfryyan, N., Alnairi, M. M., Hammoud, A., Olarinoye, I. O., Alrowaili, Z. A., & Al-Buriahi, M. S. (2023). Optical features and radiation absorption efficiency of borate glasses and the role of PbO/Eu_2O_3 substitution. Journal of Radiation Research and Applied Sciences, 16(4), 100743. https://doi.org/10.1016/j.jrras.2023.100743
27. Al Huwayz, M., Albarkaty, K. S., Alrowaili, Z. A., Olarinoye, I. O., Elqahtani, Z. M., & Al-Buriahi, M. S. (2023). Gamma, neutron, and charged particle shielding performance of ABKT glass system. Journal of Radiation Research and Applied Sciences, 16(4), 100742. https://doi.org/10.1016/j.jrras.2023.100742
28. Al-Buriahi, M. S., Sriwunkum, C., & Boukhris, I. (2021). X-and gamma-rays attenuation properties of DNA nucleobases by using FLUKA simulation code. The European Physical Journal Plus, 136(7), 776. https://doi.org/10.1140/epjp/s13360-021-01755-8